

-Supporting Information-

Controlling the Biological Fate of Micellar Nanoparticles: Balancing Stealth and Targeting

Amal J. Sivaram^{1,2,3}, Andri Wardiana¹, Sheilajen Alcantara⁵, Stefan E. Sonderegger¹, Nicholas L. Fletcher^{1,2,3}, Zachary H. Houston^{1,2,3}, Christopher B. Howard¹, Stephen M. Mahler¹, Cameron Alexander⁴, Stephen J. Kent⁵, Craig A. Bell^{1,2,3}, Kristofer J. Thurecht^{1,2,3}*

¹Australian Institute for Bioengineering and Nanotechnology, The University of Queensland, St Lucia, QLD 4072, Australia

²Centre for Advanced Imaging, The University of Queensland, St Lucia, QLD 4072, Australia

³ARC Centre of Excellence in Convergent Bio-Nano Science and Technology, and ARC Training Centre for Innovation in Biomedical Imaging Technology, The University of Queensland, St Lucia, QLD 4072, Australia

⁴School of Pharmacy, The University of Nottingham, Nottingham NG7 2RD, United Kingdom

⁵ARC Centre of Excellence in Convergent Bio-Nano Science and Technology, and the Department of Microbiology and Immunology, The University of Melbourne, at the Peter Doherty Institute for Infection and Immunity, Parkville, Victoria 3010, Australia

*Corresponding author, E-mail: k.thurecht@uq.edu.au (Kristofer J. Thurecht)

Table of Contents

Figure S1. ¹ H NMR (500 MHz, DMSO-d ₆) spectra of DBCO-p(DEGMA- <i>co</i> -MACYS) with aromatic peaks appearing between 7.3- 7.8 ppm after DBCO modification (d) along with the main peaks from p(DEGMA- <i>co</i> -MACYS) such as (a) methylene protons adjacent to the trithiocarbonate, (b) (DEGMA) side-chain protons, and (c) p(MACYS) and pDEGMA methyl protons.	5
Figure S2. Temperature dependence of hydrophobic component (p(DEGMA- <i>co</i> -MACYS)) before and after CYS modification. Normalized transmittance as a function of temperature as determined by UV analysis. The LCST onset temperature shifted from 10 °C to 16 °C after modification of PFP groups to thiols.	6
Figure S3. SDS-PAGE characterization of the hybrid conjugate (scFv-p(DEGMA- <i>co</i> -MACYS)) analysed using Coomassie blue and Cy5 channels. Lanes (left to right): Lane 1, Ladder; Lane 2, scFv; Lane 3, DBCO-p(DEGMA- <i>co</i> -MACYS); Lane 4, scFv-DBCO-p(DEGMA- <i>co</i> -MACYS). The control samples in Lane 2 and 3, scFv alone showed an intact band around 28 kDa in Coomassie blue channel whereas no detection for Cy5 containing DBCO-p(DEGMA- <i>co</i> -MACYS) in both channels. However, upon conjugation, smearing was seen in Lane 4 for both channels indicating the formation of hybrid conjugates.	6
Figure S4. DLS size distribution mPEG and scFv dispersed in PBS at 25 °C.	7
Figure S5. <i>In vitro</i> cellular association of hybrid (scFv- <i>b</i> -p(DEGMA- <i>co</i> -MACYS)) and polymer (mPEG- <i>b</i> -p(DEGMA- <i>co</i> -MACYS)) conjugates on PSMA+ and PSMA- cells measured by flow cytometry. Hybrid conjugates showed a higher association with PSMA+ cells due to higher receptor interaction.	7
Figure S6. DLS size distribution of crosslinked micelles with varying scFv densities from polymer conjugate and hybrid conjugates dispersed in PBS at 25 °C.	8
Figure S7. Zeta potential measurements of crosslinked polymer and hybrid conjugate micelles with varying scFv densities, dispersed in PBS at 25 °C.	8
Figure S8. Schematic diagram illustrating the synthesis of micelles (A5 to A75) with varying antibody densities, in which the hybrid conjugates were labelled with Cy5 dye and the polymer conjugates were labelled with rhodamine dye (RhB).	9
Figure S9. The comparison between the actual and theoretical correction factor based on the feed ratio between micelles with varying antibody densities. These values takes into consideration the amount of dye as well as possible effects related to quenching within the	

assembly. The fluorescence intensities normalised with respect to the 100% antibody-containing micelles.....9

Figure S10. DLS size distribution of polymeric micelles (A0) dispersed in PBS and serum media. The polymeric micelles retained its size after 24 h of serum treatment (10% FBS), indicating its stability.10

Figure S11. DLS size distribution of micelles dispersed in 50% serum containing media. The micelles increased in size after 48 h of incubation, indicating some interaction with serum proteins under these conditions, but no evidence of micelle fragments were observed.10

Figure S12. Fluorescence images of A0 micelles in 50% serum-containing media incubated for 0 and 48 h, obtained using the IVIS Lumina X5 imaging system. B) UV-Vis spectra of A0 micelles showing Cy5 dye peak at 647 nm after incubating in 50% serum containing media for 48 h indicating Cy5 stability.11

Figure S13. A) Flow cytometry analysis of PSMA+ cell association of Cy5-labelled micelles with varying antibody densities. B) Cellular association of micelles on PSMA+ cells after pre-incubation in free scFv ($10 \mu\text{g mL}^{-1}$) for 30 min prior to exposure to micelles.....11

Figure S14. Effect of concentration of micelles (A25 and A100) on interaction with PSMA+ cells based on mean fluorescence intensity (A) and percentage cell association of Cy5 positive cells.12

Figure S15. (A) Bar chart showing the average radiant efficiency of Cy5 signals from PSMA+ and PSMA- tumour, 48 h post iv injection of micelles with varying ligand densities of 0, 5, 10, 15, 25, 50, 75, 100% antibody content. (n = 3 per group), (B) Bar chart showing the average radiant efficiency of Cy5 signals from other major organs, 48 h post iv injection of micelles with varying ligand densities of 0, 5, 10, 15, 25, 50, 75, 100% antibody content. (n = 3 per group), (** = $p < 0.01$, *** = $p < 0.001$, **** = $p < 0.0001$).....13

Figure S16. Representative gating strategy used to isolate different murine immune cell populations in the liver and spleen. Singlets were located using side and forward scatter followed by identifying different populations based on the expression of the surface markers: CD45⁺ leucocytes; CD11b⁺ monocytes; F4/80⁺ Macrophage cells. The percentage of each cell type positive for the Cy5 micelles were then measured and an example of the gating is shown.14

Figure S17. Bar chart showing the cellular association of micelles with immune cells such as leukocytes (CD45⁺), monocytes (CD11b⁺) and macrophages (F4/80⁺) in the spleen after 24 h post iv injection of micelles with varying ligand densities of 0, 25, 50, and 100% antibody content. (n = 3 per group).....15

Figure S18. Amount of unbound serum proteins in cell culture media (containing 10% FBS) after incubating for 1 h at 37 °C, determined using Bradford assay. Values are normalised against control sample (**** = $p < 0.0001$).....15

Figure S19. Effect of antibody density on the interaction of micelles with immune cells in mice blood. Histograms show the percentage cellular association of micelles with (A) Neutrophils, (B) Monocytes, (C) B-cells, (D) T-cells at 37 °C.16

Figure S20. Representative gating strategy used to isolate different white blood cell populations. Singlets were located using side and forward scatter followed by identifying different populations based on the expression of the surface markers: CD66b+ neutrophils; CD3+ T cells; CD14+ monocytes; CD19+ B cells; and Lin-HLA-DR+ dendritic cells. The percentage of each cell type positive for the Cy5 micelles were then measured, and an example of the gating and particle association values for one sample is shown.17

Table S1. Table showing the values for Correction Factor (CF) used to compare micelles across animals. This factor was used to correct for varying concentrations of Cy5 as the different composition micelles were synthesised and takes into consideration the amount of dye as well as possible effects related to quenching within the assembly. Value normalized to the Avg Radiant Efficiency of A100 micelles.18

Minimum Information Reporting in Bio–Nano Experimental Literature (MIRIBEL) Checklist19

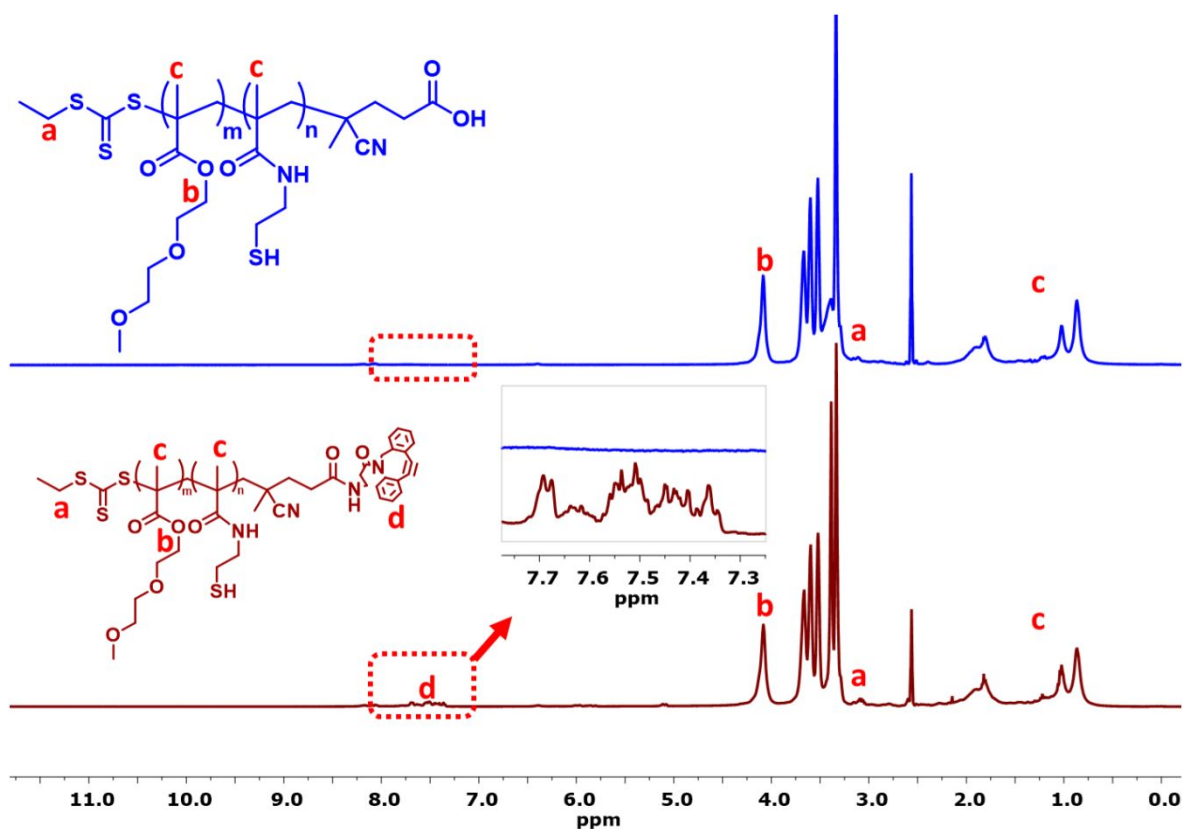


Figure S1. ¹H NMR (500 MHz, DMSO-d₆) spectra of DBCO-p(DEGMA-co-MACYS) with aromatic peaks appearing between 7.3–7.8 ppm after DBCO modification (d) along with the main peaks from p(DEGMA-co-MACYS) such as (a) methylene protons adjacent to the trithiocarbonate, (b) (DEGMA) side-chain protons, and (c) p(MACYS) and pDEGMA methyl protons.

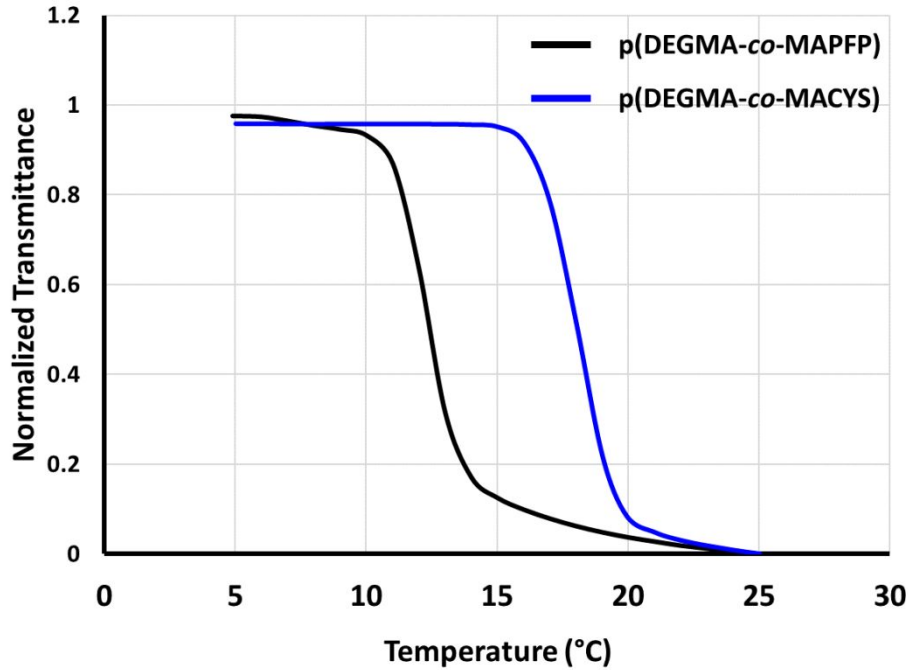


Figure S2. Temperature dependence of hydrophobic component (p(DEGMA-*co*-MACYS)) before and after CYS modification. Normalized transmittance as a function of temperature as determined by UV analysis. The LCST onset temperature shifted from 10 °C to 16 °C after modification of PFP groups to thiols.

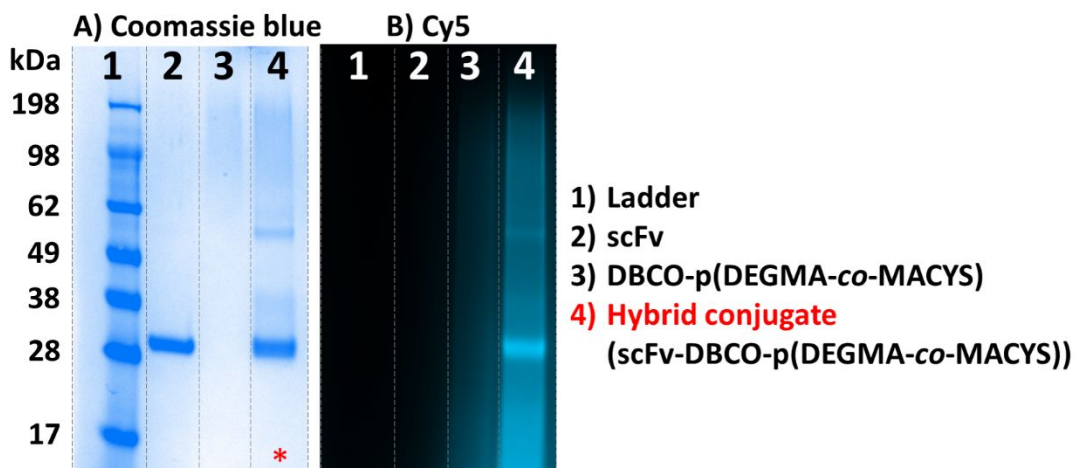


Figure S3. SDS-PAGE characterization of the hybrid conjugate (scFv-p(DEGMA-*co*-MACYS)) analysed using Coomassie blue and Cy5 channels. Lanes (left to right): Lane 1, Ladder; Lane 2, scFv; Lane 3, DBCO-p(DEGMA-*co*-MACYS); Lane 4, scFv-DBCO-p(DEGMA-*co*-MACYS). The control samples in Lane 2 and 3, scFv alone showed an intact band around 28 kDa in Coomassie blue channel whereas no detection for Cy5 containing

DBCO-p(DEGMA-*co*-MACYS) in both channels. However, upon conjugation, smearing was seen in Lane 4 for both channels indicating the formation of hybrid conjugates.

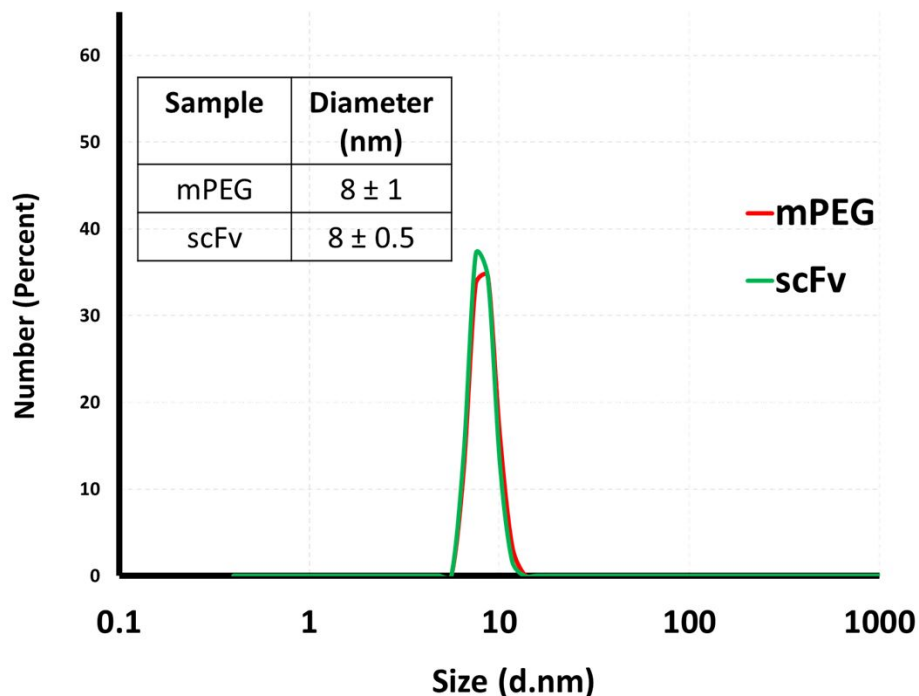


Figure S4. DLS size distribution mPEG and scFv dispersed in PBS at 25 °C.

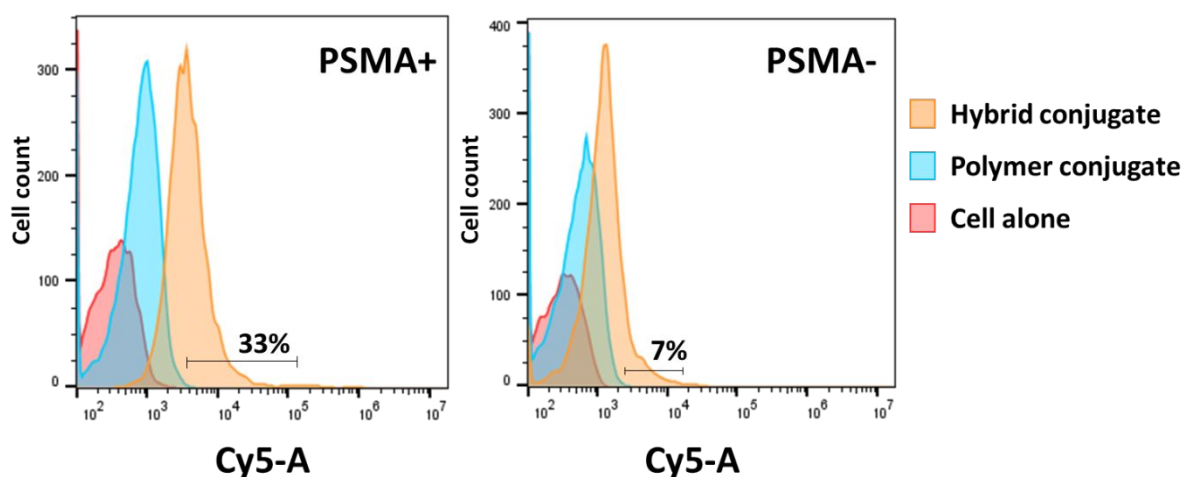


Figure S5. *In vitro* cellular association of hybrid (scFv-*b*-p(DEGMA-*co*-MACYS)) and polymer (mPEG-*b*-p(DEGMA-*co*-MACYS)) conjugates on PSMA+ and PSMA- cells measured by flow cytometry. Hybrid conjugates showed a higher association with PSMA+ cells due to higher receptor interaction.

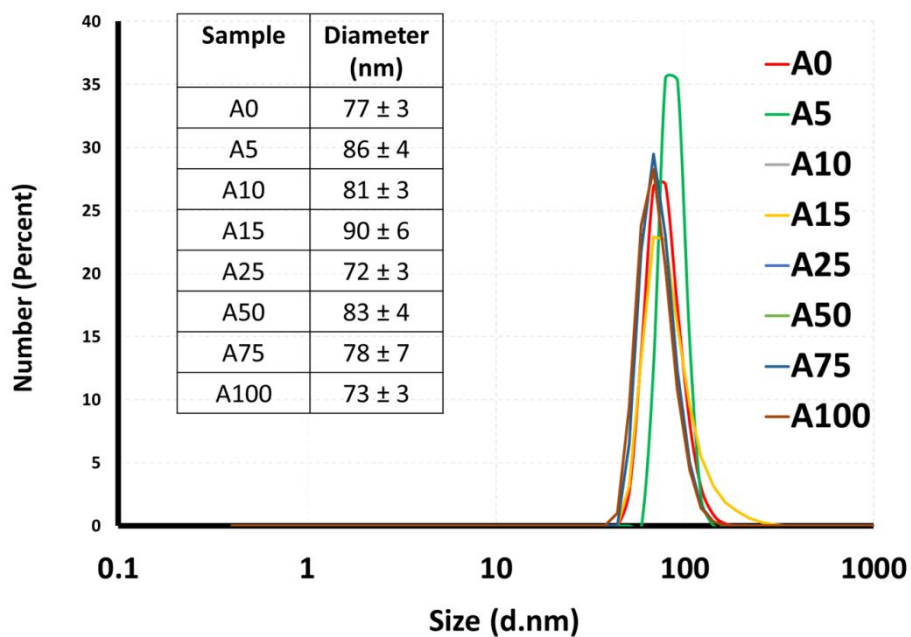


Figure S6. DLS size distribution of crosslinked micelles with varying scFv densities from polymer conjugate and hybrid conjugates dispersed in PBS at 25 °C.

Sample	Zeta potential (mV)
A0	3.9 ± 0.6
A5	4.0 ± 2.0
A10	-0.2 ± 1.0
A15	0.3 ± 2.0
A25	0.0 ± 0.7
A50	1.4 ± 0.8
A75	0.9 ± 0.2
A100	1.6 ± 0.3

Figure S7. Zeta potential measurements of crosslinked polymer and hybrid conjugate micelles with varying scFv densities, dispersed in PBS at 25 °C.

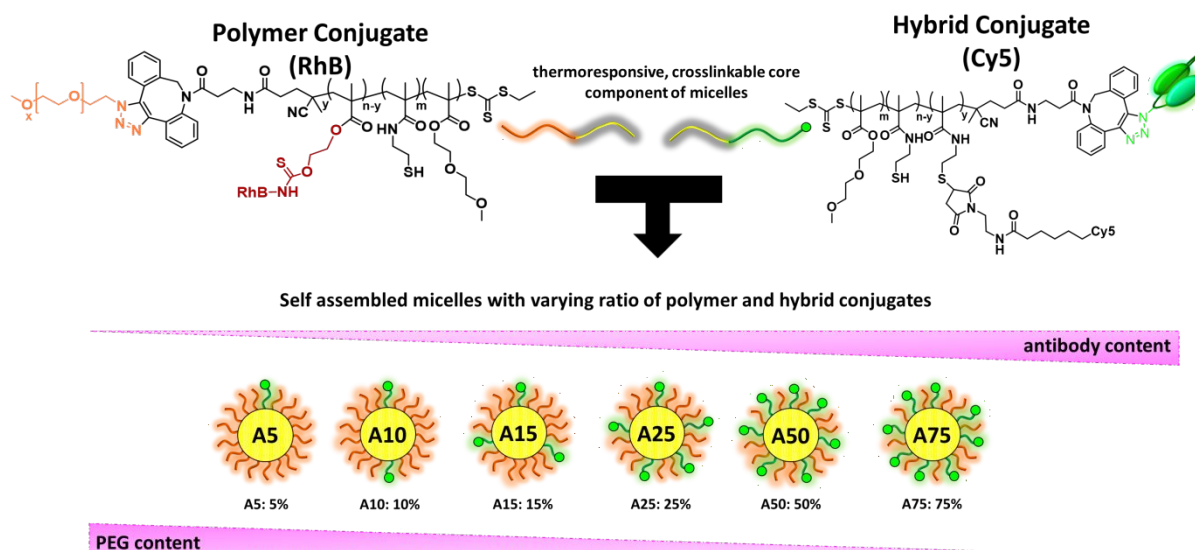


Figure S8. Schematic diagram illustrating the synthesis of micelles (A5 to A75) with varying antibody densities, in which the hybrid conjugates were labelled with Cy5 dye and the polymer conjugates were labelled with rhodamine dye (RhB).

Samples	Avg Radiant Efficiency [p/s/cm ² /sr] / [μW/cm ²]	Actual Correction factor	Theoretical Correction factor
A25	2.61E+08	3.808046	4
A50	5.22E+08	1.905118	2
A75	8.43E+08	1.179143	1.3
A100	9.94E+08	1	1

Figure S9. The comparison between the actual and theoretical correction factor based on the feed ratio between micelles with varying antibody densities. These values takes into consideration the amount of dye as well as possible effects related to quenching within the assembly. The fluorescence intensities normalised with respect to the 100% antibody-containing micelles.

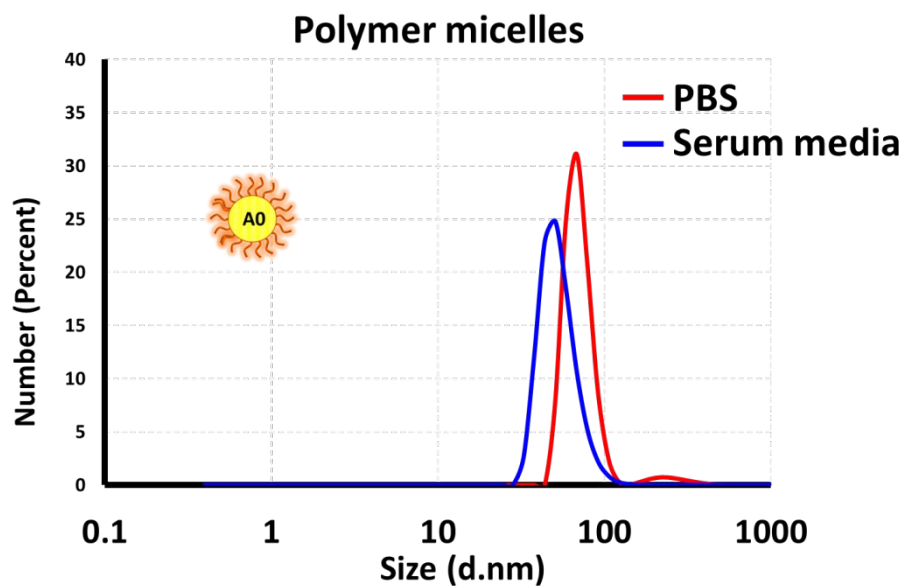


Figure S10. DLS size distribution of polymeric micelles (A0) dispersed in PBS and serum media. The polymeric micelles retained its size after 24 h of serum treatment (10% FBS), indicating its stability.

Sample	Size (nm)
A0	257 ± 60
A5	280 ± 56
A10	315 ± 60
A15	334 ± 69
A25	340 ± 66
A50	356 ± 75
A75	360 ± 57
A100	354 ± 58

Figure S11. DLS size distribution of micelles dispersed in 50% serum containing media. The micelles increased in size after 48 h of incubation, indicating some interaction with serum proteins under these conditions, but no evidence of micelle fragments was observed.

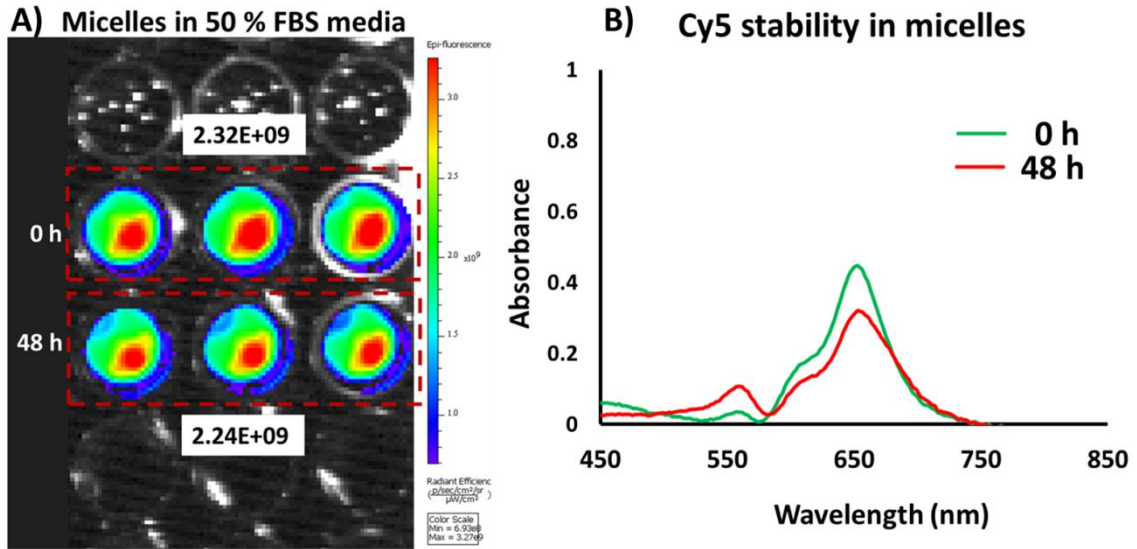


Figure S12. Fluorescence images of A0 micelles in 50% serum-containing media incubated for 0 and 48 h, obtained using the IVIS Lumina X5 imaging system. B) UV-Vis spectra of A0 micelles showing Cy5 dye peak at 647 nm after incubating in 50% serum containing media for 48 h indicating Cy5 stability.

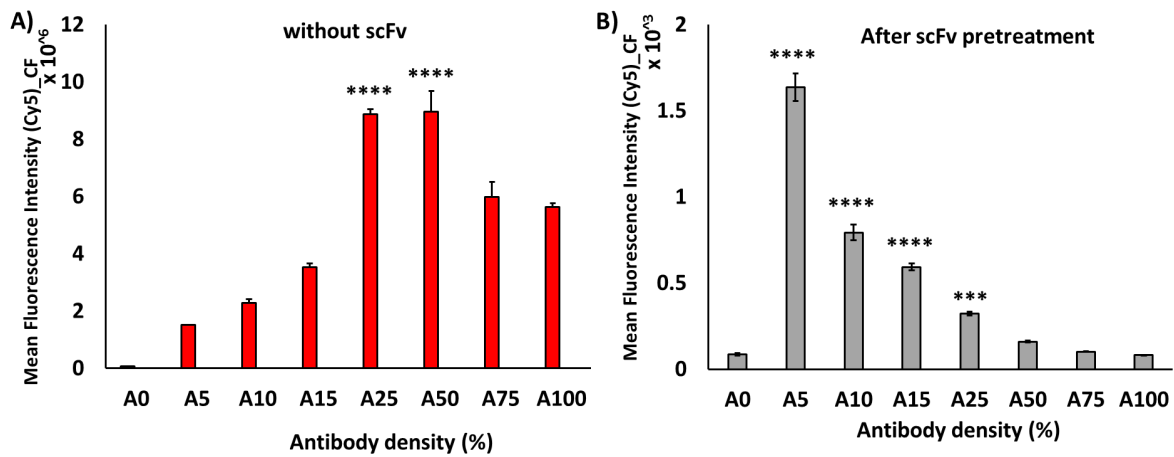


Figure S13. A) Flow cytometry analysis of PSMA+ cell association of Cy5-labelled micelles with varying antibody densities. B) Cellular association of micelles on PSMA+ cells after pre-incubation in free scFv ($10 \mu\text{g mL}^{-1}$) for 30 min prior to exposure to micelles.

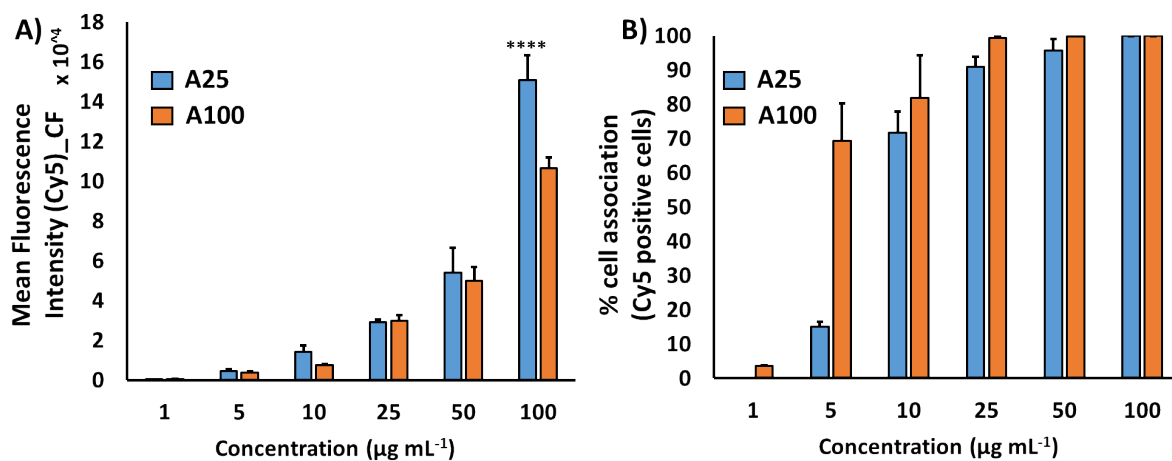


Figure S14. Effect of concentration of micelles (A25 and A100) on interaction with PSMA+ cells based on mean fluorescence intensity (A) and percentage cell association of Cy5 positive cells.

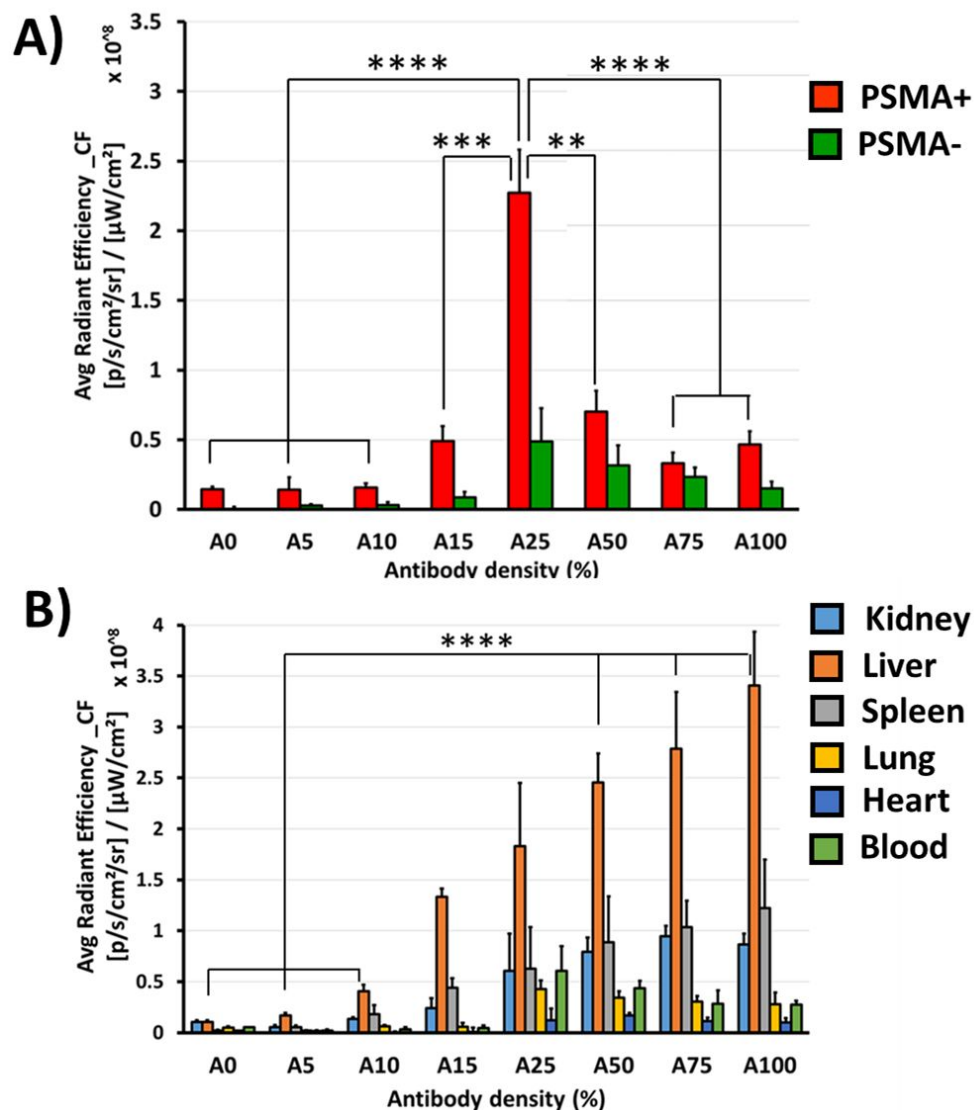


Figure S15. (A) Bar chart showing the average radiant efficiency of Cy5 signals from PSMA+ and PSMA- tumour, 48 h post iv injection of micelles with varying ligand densities of 0, 5, 10, 15, 25, 50, 75, 100% antibody content. (n = 3 per group), (B) Bar chart showing the average radiant efficiency of Cy5 signals from other major organs, 48 h post iv injection of micelles with varying ligand densities of 0, 5, 10, 15, 25, 50, 75, 100% antibody content. (n = 3 per group), (** = p < 0.01, *** = p < 0.001, **** = p < 0.0001).

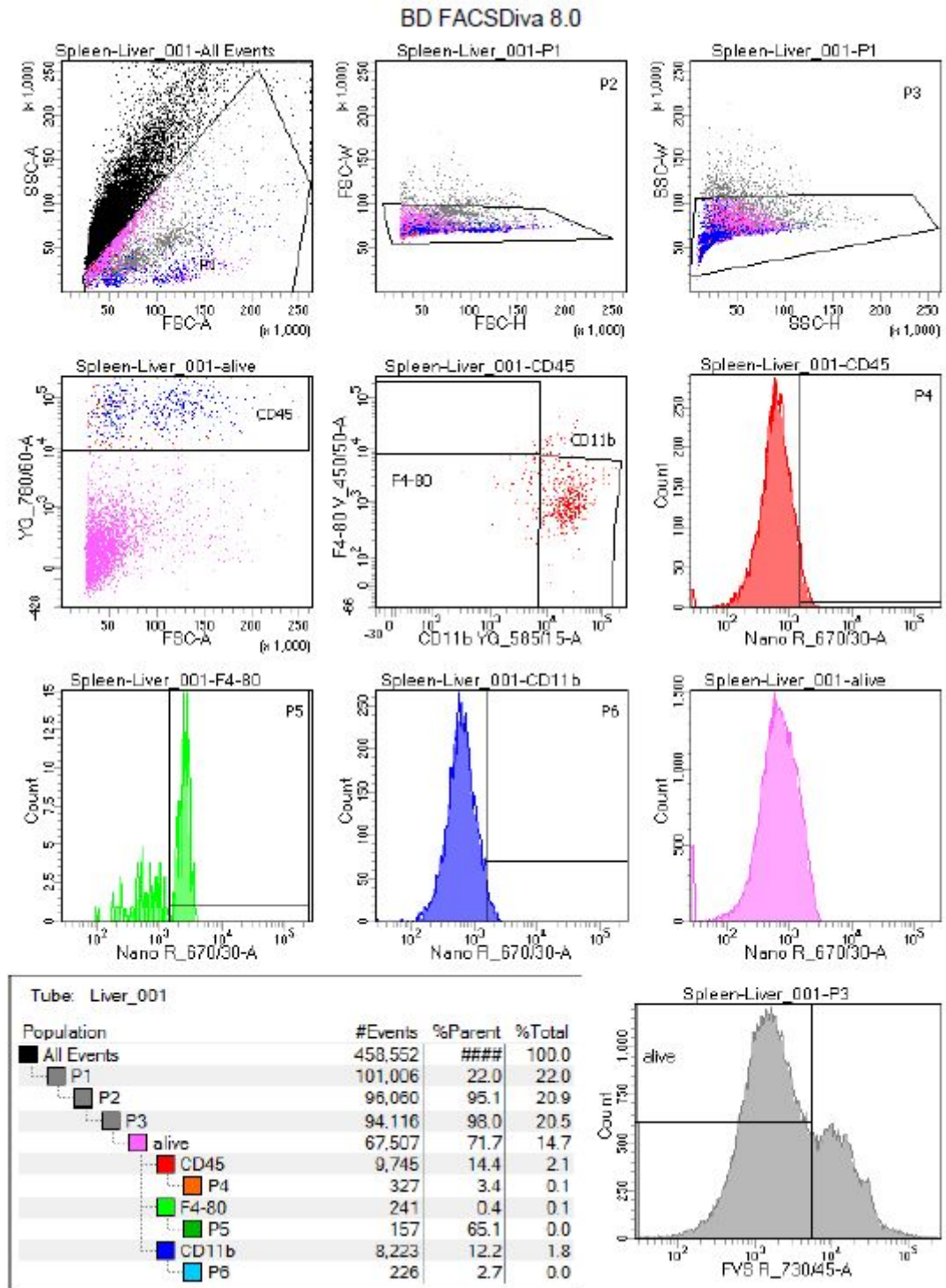


Figure S16. Representative gating strategy used to isolate different murine immune cell populations in the liver and spleen. Singlets were located using side and forward scatter followed by identifying different populations based on the expression of the surface markers: CD45⁺ leucocytes; CD11b⁺ monocytes; F4/80⁺ Macrophage cells. The percentage of each cell type positive for the Cy5 micelles were then measured and an example of the gating is shown.

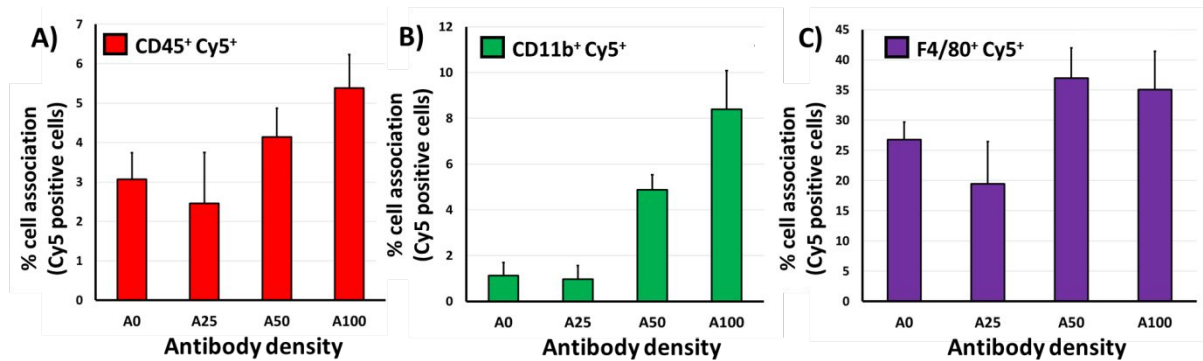


Figure S17. Bar chart showing the cellular association of micelles with immune cells such as leukocytes (CD45⁺), monocytes (CD11b⁺) and macrophages (F4/80⁺) in the spleen after 24 h post iv injection of micelles with varying ligand densities of 0, 25, 50, and 100% antibody content. (n = 3 per group).

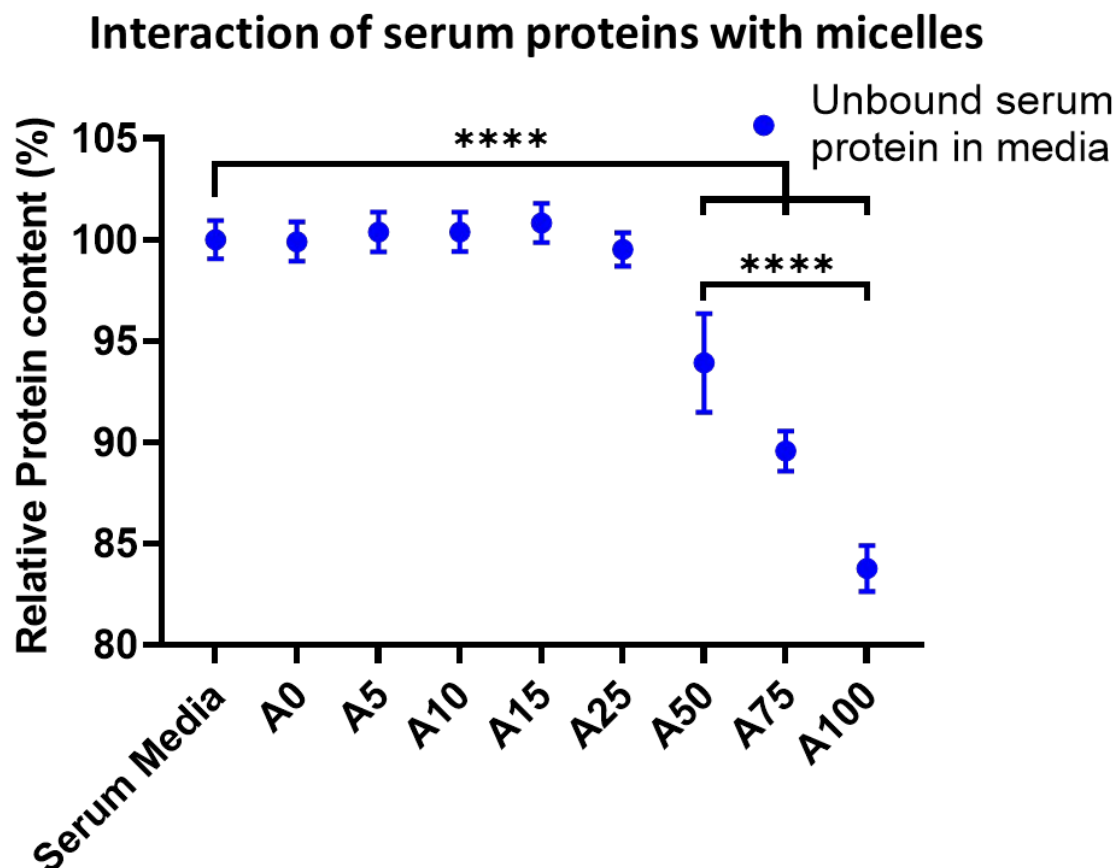


Figure S18. Amount of unbound serum proteins in cell culture media (containing 10% FBS) after incubating for 1 h at 37 °C, determined using Bradford assay. Values are normalised against control sample and compared using a two-way ANOVA followed by Tukey multicomparison test (**** = p < 0.0001).

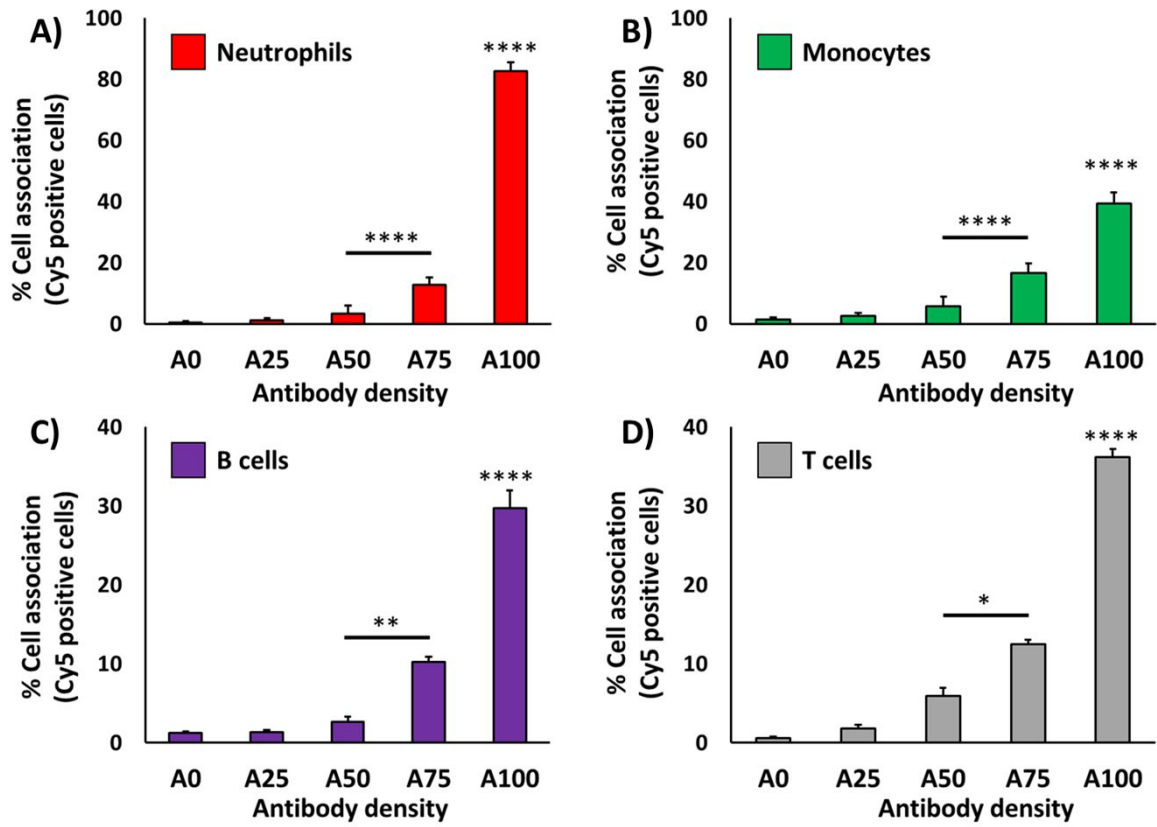


Figure S19. Effect of antibody density on the interaction of micelles with immune cells in mice blood. Histograms show the percentage cellular association of micelles with (A) Neutrophils, (B) Monocytes, (C) B-cells, (D) T-cells at 37 °C.

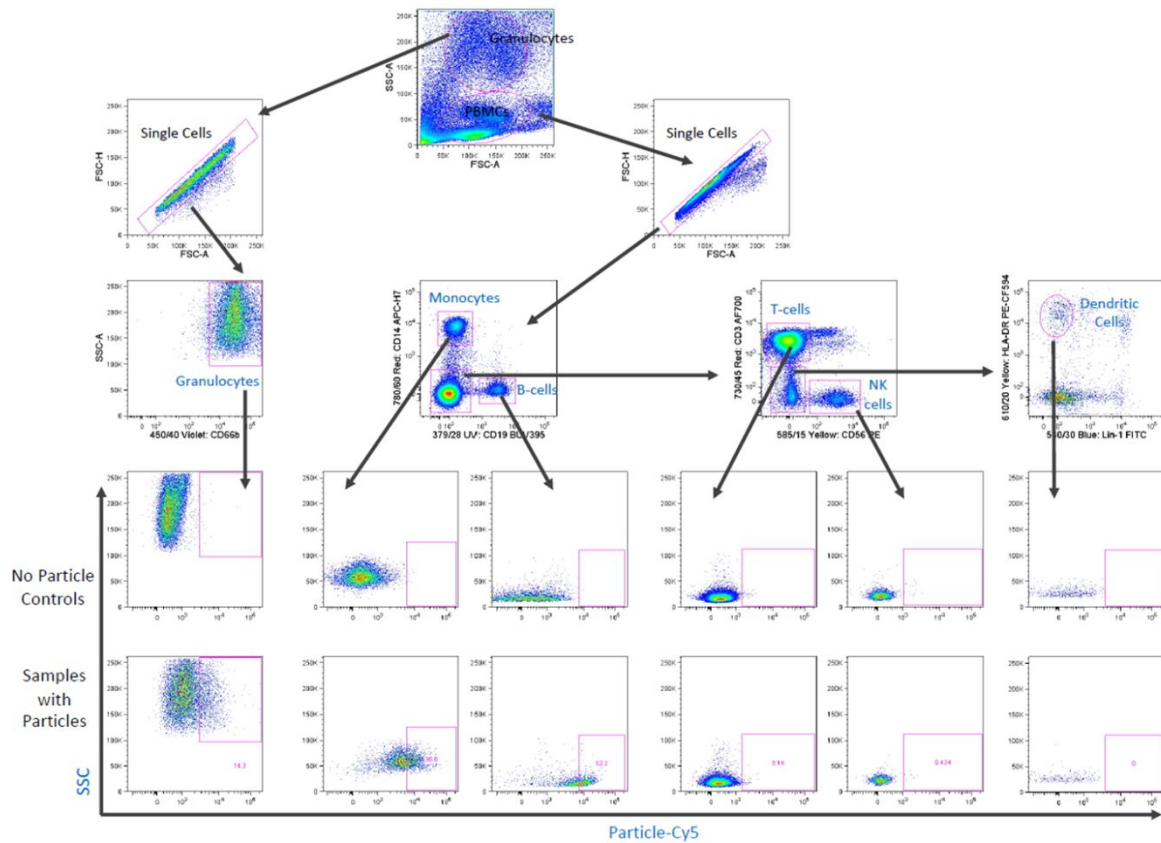


Figure S20. Representative gating strategy used to isolate different white blood cell populations. Singlets were located using side and forward scatter followed by identifying different populations based on the expression of the surface markers: CD66b+ neutrophils; CD3+ T cells; CD14+ monocytes; CD19+ B cells; and Lin-HLA-DR+ dendritic cells. The percentage of each cell type positive for the Cy5 micelles were then measured, and an example of the gating and particle association values for one sample is shown.

Table S1. Table showing the values for Correction Factor (CF) used to compare micelles across animals. This factor was used to correct for varying concentrations of Cy5 as the different composition micelles were synthesised and takes into consideration the amount of dye as well as possible effects related to quenching within the assembly. Value normalized to the Avg Radiant Efficiency of A100 micelles.

Si No.	ROI Label	Avg Radiant Efficiency [p/s/cm²/sr] / [μW/cm²]	Actual Correction Factor (CF) with respect to A100
1	A0	3.05E+09	0.325868852
2	A5	2.82E+09	0.352072
3	A10	2.31E+09	0.431006
4	A15	1.25E+09	0.793216
5	A25	2.61E+08	3.808046
6	A50	5.22E+08	1.905118
7	A75	8.43E+08	1.179143
8	A100	9.94E+08	1

Minimum Information Reporting in Bio–Nano Experimental Literature (MIRIBEL) Checklist

The MIRIBEL guidelines were introduced here: <https://doi.org/10.1038/s41565-018-0246-4>

The development of these guidelines was led by the ARC Centre of Excellence in Convergent Bio-Nano Science and Technology: <https://www.cbns.org.au/>. Any updates or revisions to this document will be made available here: <http://doi.org/10.17605/OSF.IO/SMVTF>. This document is made available under a CC-BY 4.0 license: <https://creativecommons.org/licenses/by/4.0/>.

The MIRIBEL guidelines were developed to facilitate reporting and dissemination of research in bio–nano science. Their development was inspired by various similar efforts:

- MIAME (microarray experiments): *Nat. Genet.* **29** (2001), 365; <http://doi.org/10.1038/ng1201-365>
- MIRIAM (biochemical models): *Nat. Biotechnol.* **23** (2005) 1509; <http://doi.org/10.1038/nbt1156>
- MIBBI (biology/biomedicine): *Nat. Biotechnol.* **26** (2008) 889; <http://doi.org/10.1038/nbt.1411>
- MIGS (genome sequencing): *Nat. Biotechnol.* **26** (2008) 541; <http://doi.org/10.1038/nbt1360>
- MIQE (quantitative PCR): *Clin. Chem.* **55** (2009) 611; <http://doi.org/10.1373/clinchem.2008.112797>
- ARRIVE (animal research): *PLOS Biol.* **8** (2010) e1000412; <http://doi.org/10.1371/journal.pbio.1000412>
- *Nature*'s reporting standards:
 - Life science: <https://www.nature.com/authors/policies/reporting.pdf>; e.g., *Nat. Nanotechnol.* **9** (2014) 949; <http://doi.org/10.1038/nnano.2014.287>
 - Solar cells: <https://www.nature.com/authors/policies/solarchecklist.pdf>; e.g., *Nat. Photonics* **9** (2015) 703; <http://doi.org/10.1038/nphoton.2015.233>
 - Lasers: <https://www.nature.com/authors/policies/laserchecklist.pdf>; e.g., *Nat. Photonics* **11** (2017) 139; <http://doi.org/10.1038/nphoton.2017.28>
- The “TOP guidelines”: e.g., *Science* **352** (2016) 1147; <http://doi.org/10.1126/science.aag2359>

Similar to many of the efforts listed above, the parameters included in this checklist are **not** intended to be definitive requirements; instead they are intended as ‘points to be considered’,

with authors themselves deciding which parameters are—and which are not—appropriate for their specific study.

This document is intended to be a living document, which we propose is revisited and amended annually by interested members of the community, who are encouraged to contact the authors of this document. Parts of this document were developed at the annual International Nanomedicine Conference in Sydney, Australia: <http://www.oznanomed.org/>, which will continue to act as a venue for their review and development, and interested members of the community are encouraged to attend.

After filling out the following pages, this checklist document can be attached as a “Supporting Information” document during submission of a manuscript to inform Editors and Reviewers (and eventually readers) that all points of MIRIBEL have been considered.

Supplementary Table 1. Material characterization*

Question	Yes	No
1.1 Are “ best reporting practices ” available for the nanomaterial used? For examples, see <i>Chem. Mater.</i> 28 (2016) 3535; http://doi.org/10.1021/acs.chemmater.6b01854 and <i>Chem. Mater.</i> 29 (2017) 1; http://doi.org/10.1021/acs.chemmater.6b05235		N/A
1.2 If they are available, are they used ? If not available, ignore this question and proceed to the next one.		
1.3 Are extensive and clear instructions reported detailing all steps of synthesis and the resulting composition of the nanomaterial? For examples, see <i>Chem. Mater.</i> 26 (2014) 1765; http://doi.org/10.1021/cm500632c , and <i>Chem. Mater.</i> 26 (2014) 2211; http://doi.org/10.1021/cm5010449 . Extensive use of photos, images, and videos are strongly encouraged. For example, see <i>Chem. Mater.</i> 28 (2016) 8441; http://doi.org/10.1021/acs.chemmater.6b04639	✓	
1.4 Is the size (or dimensions , if non-spherical) and shape of the nanomaterial reported?	✓	
1.5 Is the size dispersity or aggregation of the nanomaterial reported?	✓	
1.6 Is the zeta potential of the nanomaterial reported?		N/A
1.7 Is the density (mass/volume) of the nanomaterial reported?		N/A
1.8 Is the amount of any drug loaded reported? ‘Drug’ here broadly refers to functional cargos (e.g., proteins, small molecules, nucleic acids).	✓	

1.9 Is the targeting performance of the nanomaterial reported, including amount of ligand bound to the nanomaterial if the material has been functionalised through addition of targeting ligands?	✓	
1.10 Is the label signal per nanomaterial/particle reported? For example, fluorescence signal per particle for fluorescently labelled nanomaterials.	✓	
1.11 If a material property not listed here is varied, has it been quantified ?	✓	
1.12 Were characterizations performed in a fluid mimicking biological conditions ?	✓	
1.13 Are details of how these parameters were measured/estimated provided?	✓	
Explanation for No (if needed):		
1.6 Not applicable to PEG-based micelles.		
1.7 Density reported with respect to PEG and antibody component.		
1.10 Label signal per micelles reported with respect to average radiant efficiency using IVIS imaging system.		

*Ideally, material characterization should be performed in the same biological environment as that in which the study will be conducted. For example, for cell culture studies with nanoparticles, characterization steps would ideally be performed on nanoparticles dispersed in cell culture media. If this is not possible, then characteristics of the dispersant used (*e.g.*, pH, ionic strength) should mimic as much as possible the biological environment being studied.

Supplementary Table 2. Biological characterization*

Question	Yes	No
2.1 Are cell seeding details , including number of cells plated, confluency at start of experiment, and time between seeding and experiment reported?	✓	
2.2 If a standardised cell line is used, are the designation and source provided?	✓	
2.3 Is the passage number (total number of times a cell culture has been subcultured) known and reported?		✓
2.4 Is the last instance of verification of cell line reported? If no verification has been performed, is the time passed and passage number since acquisition from trusted source (<i>e.g.</i> , ATCC or ECACC) reported? For information, see <i>Science</i> 347 (2015) 938; http://doi.org/10.1126/science.347.6225.938		✓
2.5 Are the results from mycoplasma testing of cell cultures reported?		✓

2.6 Is the background signal of cells/tissue reported? (<i>E.g.</i> , the fluorescence signal of cells without particles in the case of a flow cytometry experiment.)		✓
2.7 Are toxicity studies provided to demonstrate that the material has the expected toxicity, and that the experimental protocol followed does not?		N/A
2.8 Are details of media preparation (type of media, serum, any added antibiotics) provided?	✓	
2.9 Is a justification of the biological model used provided? For examples for cancer models, see <i>Cancer Res.</i> 75 (2015) 4016; http://doi.org/10.1158/0008-5472.CAN-15-1558 , and <i>Mol. Ther.</i> 20 (2012) 882; http://doi.org/10.1038/mt.2012.73 , and <i>ACS Nano</i> 11 (2017) 9594; http://doi.org/10.1021/acsnano.7b04855	✓	
2.10 Is characterization of the biological fluid (<i>ex vivo/in vitro</i>) reported? For example, when investigating protein adsorption onto nanoparticles dispersed in blood serum, pertinent aspects of the blood serum should be characterised (<i>e.g.</i> , protein concentrations and differences between donors used in study).		N/A
2.11 For animal experiments , are the ARRIVE guidelines followed? For details, see <i>PLOS Biol.</i> 8 (2010) e1000412; http://doi.org/10.1371/journal.pbio.1000412	✓	

Explanation for **No** (if needed):

2.3 & 2.4 The cells were between passages 15-25 since receipt from ATCC.

2.5 Cells were mycoplasma tested regularly and were last reported as negative as of 18/09/2018.

2.6 Cell autofluorescence was not pertinent, being accounted for during experimental set-up.

2.7 Not the primary objective of the current study and the concentrations used didn't show any toxicity.

*For *in vitro* experiments (*e.g.*, cell culture), *ex vivo* experiments (*e.g.*, in blood samples), and *in vivo* experiments (*e.g.*, animal models). The questions above that are appropriate depend on the type of experiment conducted.

Supplementary Table 3. Experimental details*

Question	Yes	No
3.1 For cell culture experiments: are cell culture dimensions including type of well, volume of added media , reported? Are cell types (<i>i.e.</i> ; adherent vs suspension) and orientation (if non-standard) reported?	✓	

3.2 Is the dose of material administered reported? This is typically provided in nanomaterial mass, volume, number, or surface area added. Is sufficient information reported so that regardless of which one is provided, the other dosage metrics can be calculated (<i>i.e.</i> using the dimensions and density of the nanomaterial)?	✓	
3.3 For each type of imaging performed, are details of how imaging was performed provided, including details of shielding, non-uniform image processing , and any contrast agents added?	✓	
3.4 Are details of how the dose was administered provided, including method of administration, injection location, rate of administration , and details of multiple injections ?	✓	
3.5 Is the methodology used to equalise dosage provided?	✓	
3.6 Is the delivered dose to tissues and/or organs (<i>in vivo</i>) reported, as % injected dose per gram of tissue (%ID g ⁻¹)?		✓
3.7 Is mass of each organ/tissue measured and mass of material reported?		✓
3.8 Are the signals of cells/tissues with nanomaterials reported? For instance, for fluorescently labelled nanoparticles, the total number of particles per cell or the fluorescence intensity of particles + cells, at each assessed timepoint.	✓	
3.9 Are data analysis details , including code used for analysis provided?	✓	
3.10 Is the raw data or distribution of values underlying the reported results provided? For examples, see <i>R. Soc. Open Sci.</i> 3 (2016) 150547; http://doi.org/10.1098/rsos.150547 , https://opennessinitiative.org/making-your-data-public/ , http://journals.plos.org/plosone/s/data-availability , and https://www.nature.com/sdata/policies/repositories	✓	
Explanation for No (if needed):		

* The use of protocol repositories (*e.g.*, *Protocol Exchange* <http://www.nature.com/protocolexchange/>) and published standard methods and protocols (*e.g.*, *Chem. Mater.* **29** (2017) 1; <http://doi.org/10.1021/acs.chemmater.6b05235>, and *Chem. Mater.* **29** (2017) 475; <http://doi.org/10.1021/acs.chemmater.6b05481>) are encouraged.